CD11b regulates obesity-induced insulin resistance via limiting alternative activation and proliferation of adipose tissue macrophages

Chunxing Zheng[a], Qian Yang[a], Chunliang Xu[a], Peishun Shou[a], Jianchang Cao[a], Menghui Jiang[a], Qing Chen[a], Gang Cao[a], Yanyan Han[a], Fengying Li[a], Wei Cao[a], Liying Zhang[b], Li Zhang[c], Yufang Shi[a,b,d,1], and Ying Wang[a,1]

[a]Key Laboratory of Stem Cell Biology, Institute of Health Sciences, Shanghai Institutes for Biological Sciences, Chinese Academy of Sciences/Shanghai Jiao Tong University School of Medicine, Shanghai 200031, China; [b]The First Affiliated Hospital of Soochow University, Institutes for Translational Medicine, Soochow University, Suzhou 215006, China; [c]Center for Vascular and Inflammatory Diseases, Department of Physiology, University of Maryland School of Medicine, Baltimore, MD 21201; and [d]Child Health Institute of New Jersey, Rutgers-Robert Wood Johnson Medical School, New Brunswick, NJ 08901

Edited by Ruslan Medzhitov, Yale University School of Medicine, New Haven, CT, and approved November 24, 2015 (received for review January 8, 2015)

Obesity-associated inflammation is accompanied by the accumulation of adipose tissue macrophages (ATMs), which is believed to predispose obese individuals to insulin resistance. CD11b (integrin α_M) is highly expressed on monocytes and macrophages and is critical for their migration and function. We found here that high-fat diet–induced insulin resistance was significantly reduced in CD11b-deficient mice. Interestingly, the recruitment of monocytes to adipose tissue is impaired when CD11b is deficient, although the cellularity of ATMs in CD11b-deficient mice is higher than that in wild-type mice. We further found that the increase in ATMs is caused mainly by their vigorous proliferation in the absence of CD11b. Moreover, the proliferation and alternative activation of ATMs are regulated by the IL-4/STAT6 axis, which is inhibited by CD11b through the activity of phosphatase SHP-1. Thus, CD11b plays a critical role in obesity-induced insulin resistance by limiting the proliferation and alternative activation of ATMs.

integrin CD11b | macrophage proliferation | alternative activation | obesity | insulin resistance

Obesity is associated with chronic inflammation characterized by progressive accumulation of immune cells in adipose tissue. Cytokines secreted by these immune cells, such as TNF-α, have been demonstrated to augment adipose tissue inflammation and consequentially induce insulin resistance (1, 2). As one of the major cell types that contribute to the proinflammatory response, macrophages are central players in obesity-related inflammation (3, 4). This heterogeneous cell population possesses broad plasticity that can be influenced by the local microenvironment. Changes in macrophage properties play distinct roles in regulating inflammation and also metabolic responses (5, 6). Classically activated macrophages (CAMs) secrete proinflammatory cytokines such as TNF-α, IL-6, and IL-1 (7). The accumulation of CAMs in adipose tissue exacerbates the development of obesity and subsequent tissue inflammation and insulin resistance. On the other hand, resident macrophages in adipose tissue of lean mice display a phenotype of alternatively activated macrophages (AAMs) with high expression of IL-10, Ym1/chitinase3-like3, and arginase1 (8). It has been reported that AAMs driven by IL-4 and IL-13 could improve insulin sensitivity (9, 10). Thus, differential accumulation of these two macrophage populations could result in distinct metabolic states and could influence the progression of insulin resistance.

Traditionally, the accumulation of macrophages is considered as the migration of monocytes to inflammatory sites and subsequent differentiation into macrophages (5). One of the molecules that control monocytes immigration is integrin α_M (CD11b), which combines with integrin β_2 (CD18) to form MAC-1 (integrin $\alpha_M\beta_2$). MAC-1 is well known for its role in regulating leukocyte transmigration through endothelial cells (11, 12). The function of CD11b is dependent on a cascade of inside–out and outside–in activation signaling processes. The activation of tyrosine kinases, especially members of the Src family, is indispensable for the outside–in signaling of different integrins (13). In addition to its role in regulating leukocyte adhesion and migration, CD11b has been reported to modulate various aspects of immune responses. Our previous studies showed that CD11b on antigen-presenting cells plays a critical role in promoting oral tolerance by inhibiting Th17 differentiation (14). Moreover, CD11b also has been shown to suppress Toll-like receptor–initiated signals in macrophages and thus to protect animals from endotoxic shock (15). Interestingly, activation of CD11b impedes the accumulation of lipid in macrophages and the formation of foam cells in the presence of IL-13 (16). Its negative regulation of the immune response also can be observed in B cells, because CD11b has been shown to inhibit the autoreactive B-cell response in systemic lupus erythematous (17). Importantly, CD11b is found to be involved in regulating body fat deposition (18); however, the effect of CD11b in obesity-induced insulin resistance has not been reported. In the present study, we show that CD11b is important for the influx of monocytes to adipose tissue during the development of obesity. Surprisingly, the accumulation of macrophages in the adipose tissue of CD11b-deficient mice is significantly increased compared with that in wild-type mice. We further demonstrated that CD11b deficiency promotes in situ proliferation of adipose tissue macrophages (ATMs), a process mediated by the IL-4/STAT6 signaling pathway. The infiltrated ATMs in CD11b-deficient mice phenotypically resemble AAMs. Depletion of these ATMs reversed the reduction of

Significance

Obesity is associated with long-term low-grade inflammation characterized by the accumulation of adipose tissue macrophages (ATMs). One important molecule that regulates the migration of monocytes/macrophages is CD11b (integrin α_M). Here we show an unexpected role of CD11b in modulating the IL-4/STAT6 signaling in macrophages, thereby limiting IL-4/STAT6–mediated proliferation and alternative activation of ATMs. In the absence of CD11b, there is an increase in ATM in situ proliferation and an enhancement of alternatively polarized phenotypes. Importantly, the alternatively activated ATMs attenuate obesity-related insulin resistance in CD11b-deficient mice. These results reveal a previously unidentified physiological function of CD11b, which could be a therapeutic target for insulin resistance.

Author contributions: C.Z., Y.S., and Y.W. designed research; C.Z., Q.Y., J.C., M.J., Q.C., G.C., Y.H., F.L., W.C., and Liying Zhang performed research; C.Z., Q.Y., C.X., P.S., Li Zhang, and Y.W. analyzed data; and C.Z., Y.S., and Y.W. wrote the paper.

The authors declare no conflict of interest.

This article is a PNAS Direct Submission.

Freely available online through the PNAS open access option.

[1]To whom correspondence may be addressed. Email: yufangshi@sibs.ac.cn or yingwang@sibs.ac.cn.

This article contains supporting information online at www.pnas.org/lookup/suppl/doi:10.1073/pnas.1500396113/-/DCSupplemental.

insulin resistance. Thus, our studies revealed a previously unidentified role of CD11b in regulating macrophage cellularity and function in adipose tissue and insulin resistance.

Results

CD11b Deficiency Reduces Insulin Resistance While Increasing Macrophage Cellularity in Adipose Tissue. Integrin CD11b on macrophages plays important roles in regulating migration and function. To investigate the impact of this molecule on obesity-related insulin resistance, we induced obesity using a high-fat diet (HFD) in CD11b-deficient mice and wild-type controls. As in previous reports (18), with the same amount of food intake (Fig. S1*A*), CD11b$^{-/-}$ mice gained significantly more body weight than control mice (Fig. S1*B*) and showed increased amounts of adipose tissue (Fig. S1*C*). Interestingly, these more obese CD11b$^{-/-}$ mice exhibited better glucose tolerance (Fig. 1*A* and Fig. S1 *D* and *E*), less insulin resistance (Fig. 1*B*), and significantly lower serum insulin concentration (Fig. S1*F*). Furthermore, the attenuation of insulin resistance also was observed in HFD-treated wild-type mice that had been reconstituted with CD11b$^{-/-}$ bone marrow but not in those reconstituted with wild-type bone marrow (Fig. 1 *C* and *D* and Fig. S1*G*).

Because long-term low-grade inflammation during obesity is believed to be critical for the development of insulin resistance, we examined leukocytes in adipose tissue histologically and flow cytometrically. To our surprise, we found that the leukocyte cellularity was significantly higher in the adipose tissue of CD11b$^{-/-}$ mice than in that of wild-type mice (Fig. 1*E*). Further immunofluorescence staining (Fig. 1*F*) and flow cytometric analysis (Fig. 1*G* and Fig. S2 *A* and *B*) revealed that the increase in leukocytes was mainly an increase in macrophages, not T or B cells.

The Increase in ATMs Is Not Caused by Enhanced Monocyte Immigration. The recruitment and migration of monocytes is essential for the inflammatory response during injury, infection, and autoimmune disorders. CD11b is highly expressed on monocytes and is critical for the migration of these cells to inflammatory sites (19). To investigate the role of CD11b in mediating the migration of monocytes into the adipose tissue of obese mice, we performed competitive constitution experiments in syngeneic mice. Monocytes were isolated from wild-type and CD11b$^{-/-}$ mice on the CD45.2 background using a negative selection kit. The isolation process resulted in a great enrichment of monocytes (Ly6C^{+}CD115^{+}), from 5 to >70% (Fig. S3*A*). Recipient CD45.1 mice were fed an HFD for 10 wk and then were transfused with a mixture of monocytes isolated from CD45.2 wild-type mice and CD45.2 CD11b$^{-/-}$ mice (Fig. 2*A* and Fig. S3*B*). Twenty-four hours later, macrophages derived from donor monocytes were detected in the adipose tissue of recipient mice (Fig. 2*B*), and 0.11% of the ATMs were derived from transfused monocytes. Donor macrophages derived from wild-type and CD11b$^{-/-}$ monocytes can be distinguished by CD11b labeling (Fig. 2*C*). Within 24 h, Eighty percent of the donor monocyte-derived ATMs in epididymal adipose depots (representative of visceral adipose tissue) were from wild-type monocytes, and 20% were from CD11b$^{-/-}$ monocytes (Fig. 2 *C* and *D*). The same pattern of donor ATMs was observed in inguinal adipose depots (representative of s.c. adipose tissue) (Fig. 2 *E* and *F*). At the same time point, however, equal percentages of wild-type

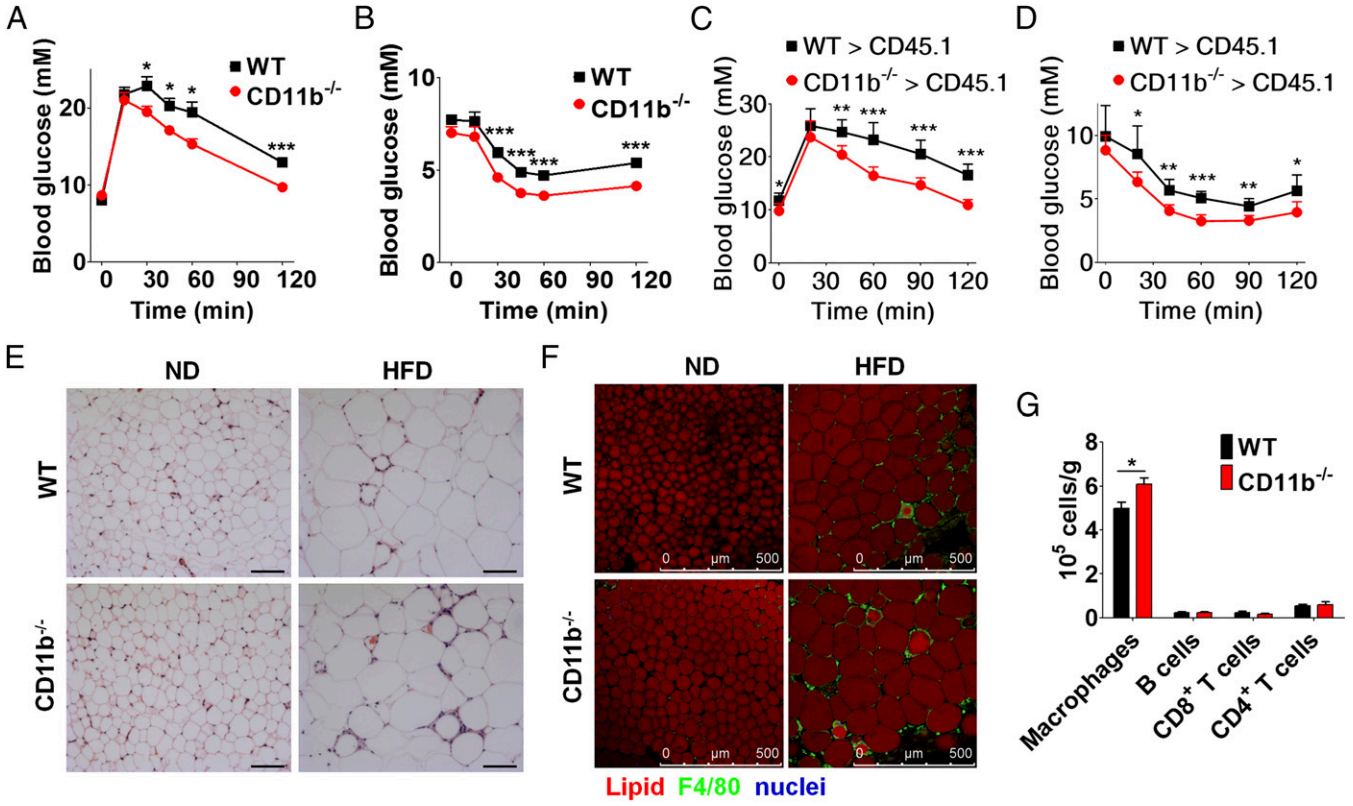

Fig. 1. CD11b deficiency reduces insulin resistance while increasing ATMs. (*A* and *B*) Glucose-tolerance test (*A*) and insulin-tolerance test (*B*) in HFD-treated wild-type and CD11b$^{-/-}$ mice (n = 9–10 mice in each group). Error bars represent means ± SEM. *P < 0.05, **P < 0.01. (*C* and *D*) Glucose-tolerance test (*C*) and insulin-tolerance test (*D*) in HFD-treated wild-type (CD45.1) mice that were reconstituted with wild-type or CD11b$^{-/-}$ bone marrow (n = 6–8 mice in each group). Error bars represent means ± SEM. *P < 0.05, ** P < 0.01, *** P < 0.001. (*E*) H&E staining of epididymal adipose tissue showing leukocyte accumulation. (Scale bars, 100 μM.) (*F*) Immunofluorescence showing macrophage accumulation in epididymal adipose tissue. (Scale bars, 500 μM.) (*G*) Total numbers of different immune cells per gram of epididymal adipose tissue from HFD-treated mice were analyzed by flow cytometry. Data are shown as means ± SEM (n = 4 mice in each group). *P < 0.05.

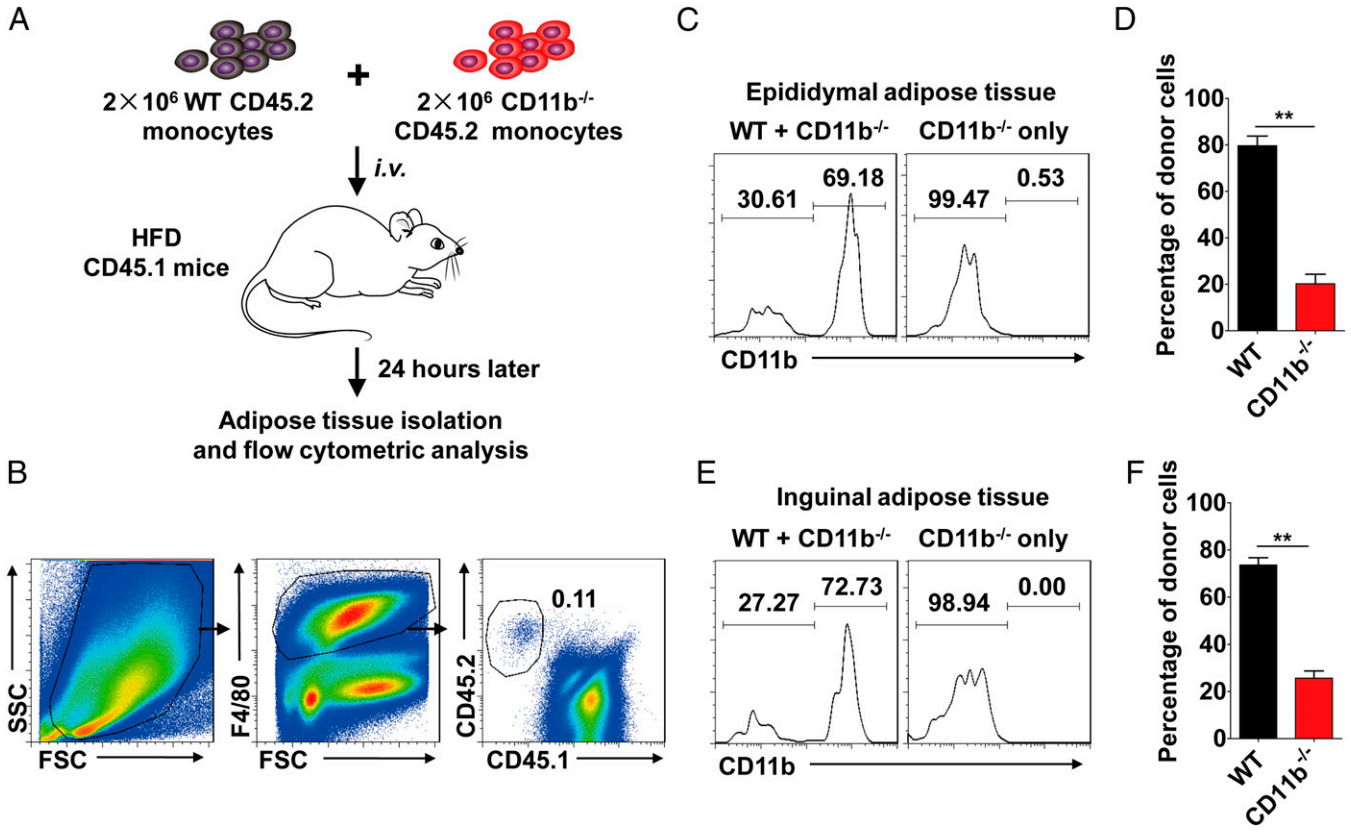

Fig. 2. CD11b deficiency impairs the migration of monocytes to adipose tissue. (*A*) Schematic representation of competitive monocyte constitution. Two million monocytes isolated from the bone marrow of CD45.2 wild-type mice were mixed with 2×10^6 monocytes from CD45.2 CD11b$^{-/-}$ mice and were injected i.v. into HFD-treated CD45.1 mice. Twenty-four hours later the stromal cell fraction was analyzed for CD45, F4/80, and CD11b. (*B*) Detection of ATMs derived from donor monocytes by flow cytometry based on F4/80 and CD45.2. (*C* and *E*) Proportion of ATMs derived from wild-type and CD11b$^{-/-}$ monocytes in epididymal adipose tissue (*C*) and inguinal adipose tissue (*E*). Recipient mice were injected with only CD11b$^{-/-}$ monocytes as a gating control (*Left*) or with wild-type and CD11b$^{-/-}$ monocytes (*Right*). (*D* and *F*) Summarizing the proportion of ATMs derived from wild-type and CD11b$^{-/-}$ monocytes in epididymal adipose tissue (*D*) and inguinal adipose tissue (*F*) in mice of four independent experiments. Data are shown as mean ± SEM; $^{**}P < 0.01$, paired *t*-test.

donor monocytes and CD11b$^{-/-}$ donor monocytes were found in the peripheral blood of recipient mice (Fig. S3 *C* and *D*), excluding the possibility that the observed difference in the recruitment to adipose tissue is caused by differential survival or clearance of monocytes from the two types of mice. These results demonstrated that CD11b deficiency greatly compromises the ability of monocytes to influx into the adipose tissue of obese mice.

The observation of less monocyte immigration but more ATM accumulation contradicts the general notion that the influx of monocytes determines the degree of macrophage accumulation. Two possible reasons might explain the paradoxical enhancement of ATM accumulation when the immigration of monocytes is actually reduced. One is that the life span of macrophages is prolonged by CD11b deficiency. In fact, it has been reported that CD11b engagement promotes the proapoptotic signals and that CD11b/CD18 promoted phagocytosis-induced apoptosis of neutrophils (20, 21). To determine whether there is a decrease in cell death in CD11b$^{-/-}$ ATMs, we performed a TUNEL assay. We found that cell death of ATMs from both wild-type and CD11b$^{-/-}$ mice is negligible, and we did not find any difference in the level of cell death in ATMs from wild-type and CD11b$^{-/-}$ mice (Fig. S4). The other possible solution for the increase in ATMs in CD11b$^{-/-}$ mice is enhanced proliferation.

Increased ATM Proliferation in Obese CD11b-Deficient Mice. Previous studies demonstrated that the accumulation of tissue macrophages during inflammation can result from the expansion of the resident population (22), suggesting that enhanced in situ proliferation of macrophages can lead to the observed increase in ATM accumulation in CD11b$^{-/-}$ mice. To examine whether ATMs could proliferate locally, we treated mice receiving either a normal diet or an HFD with 5-ethynyl-2′-deoxyuridine (EdU) for 3 h and then analyzed macrophages with EdU incorporation in the epididymal adipose tissue by flow cytometry. EdU-incorporated ATMs were increased after HFD treatment (Fig. S5*A*). It is worth noting that there are no detectable EdU-incorporated monocytes in blood (Fig. S2*C* and Fig. S5*B*), suggesting a special property of ATMs and excluding the possibility that the EdU-incorporated ATMs in adipose tissue were from circulation. We also checked Ki67, a hallmark of cells in the cell cycle, and found that Ki67$^+$ macrophages from epididymal adipose tissue were greatly increased in HFD-treated mice (Fig. S5*C*). These experiments showed that an HFD could induce ATM proliferation in wild-type mice.

We hypothesized that CD11b deficiency could lead to a further increase in the proliferation of macrophages in the adipose tissue in mice on an HFD. This increase accounts for the increased ATM accumulation in obese CD11b$^{-/-}$ mice. By comparing Ki67$^+$ ATMs in wild-type mice and CD11b$^{-/-}$ mice on an HFD, we found a dramatic increase in Ki67$^+$ macrophages in the adipose tissue of CD11b$^{-/-}$ mice (Fig. 3 *A* and *B*). We also analyzed Ki67 expression in ATMs from HFD-treated CD11b$^{-/-}$ mice and their heterozygous littermates and found a significant increase in Ki67 expression in CD11b$^{-/-}$ mice (Fig. S5*D*). To determine in situ whether the Ki67$^+$ macrophages are indeed in adipose tissue, we carried out whole-mount staining on epididymal adipose tissue and localized those Ki67$^+$ macrophages in the crown-like-structures

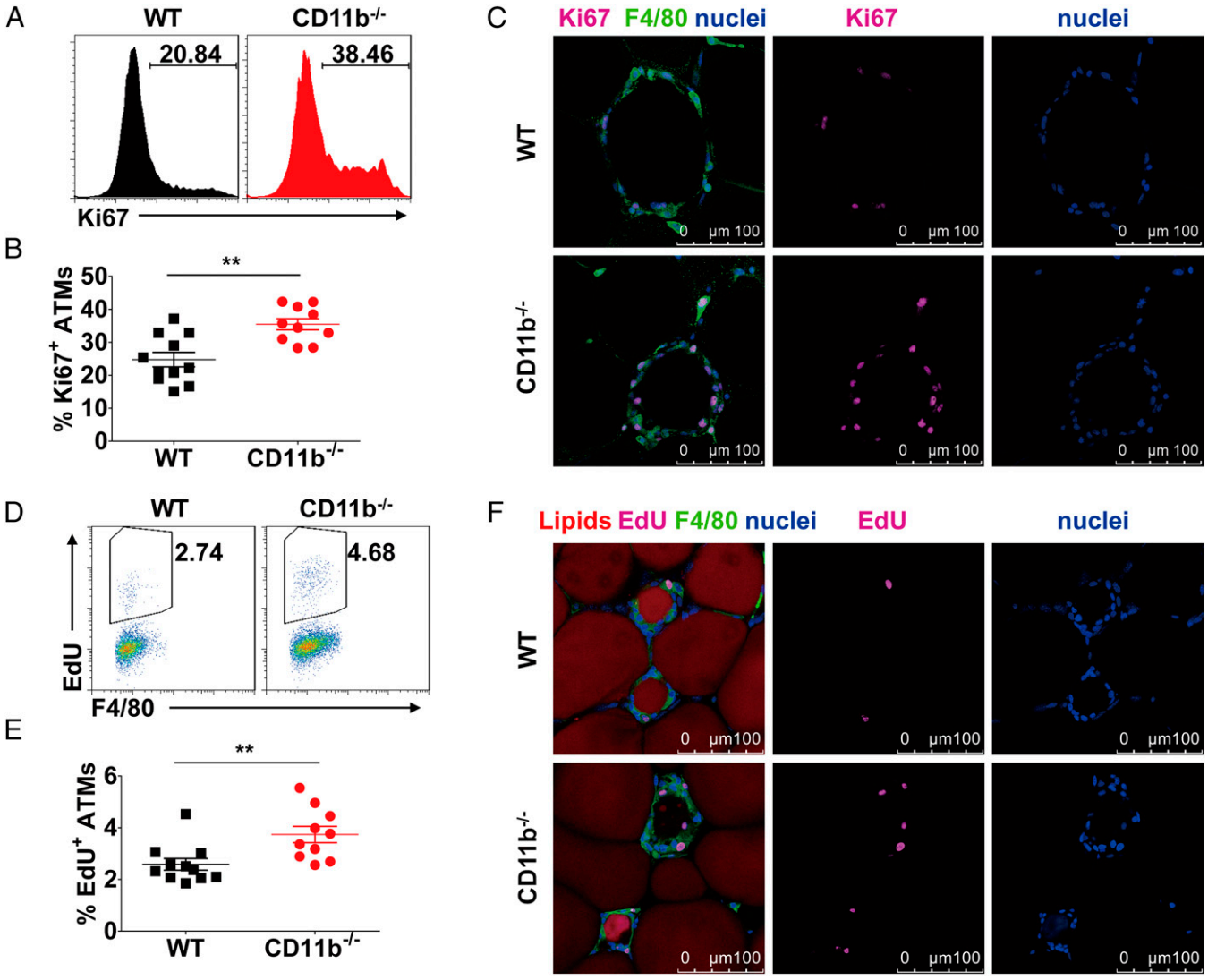

Fig. 3. CD11b deficiency promotes in situ proliferation of ATMs during obesity. (*A*) Flow cytometric analysis of Ki67 expression in ATMs from epididymal adipose tissue of wild-type and CD11b$^{-/-}$ mice on an HFD. ATMs were gated on CD45^{+}F4/80^{hi}Siglec-F^{-} as shown in Fig. S2*A*. (*B*) ATM proliferation as detected by Ki67 expression in all mice from two independent experiments. Data are shown as means ± SEM. $^{**}P < 0.01$. (*C*) Immunofluorescence staining for Ki67^{+} ATMs in epididymal adipose tissue of wild-type and CD11b$^{-/-}$ mice on an HFD. (Scale bars, 100 μM.) (*D*) Flow cytometric analysis of EdU incorporation in ATMs from epididymal adipose tissue of wild-type and CD11b$^{-/-}$ mice on an HFD. Mice were pulsed with 10 μg EdU per gram of body weight for 3 h. (*E*) ATM proliferation as detected by EdU in all mice from two independent experiments. Data are shown as mean ± SEM. $^{**}P < 0.01$. (*F*) Immunofluorescence staining for EdU-incorporated ATMs in the epididymal adipose tissue of wild-type and CD11b$^{-/-}$ mice on an HFD. (Scale bars, 100 μM.)

(CLSs) formed by accumulated macrophages. We found that Ki67^{+} macrophages are increased in the CLSs of adipose tissue from CD11b$^{-/-}$ mice (Fig. 3*C*). We also performed the EdU incorporation assay on HFD-treated wild-type and CD11b$^{-/-}$ mice and observed significantly augmented EdU incorporation in CD11b$^{-/-}$ ATMs (Fig. 3 *D* and *E*). Those EdU-incorporated ATMs are sporadic in adipose tissue and exhibit CLS localization in close proximity to other macrophages (Fig. 3*F*). Thus, CD11b plays a negative role in regulating macrophage proliferation in the adipose tissue of obese mice.

ATM Proliferation Depends on the IL-4/STAT6 Signaling Axis. Several cytokines, including IL-4, macrophage colony-stimulating factor (M-CSF), and monocyte chemotactic protein 1 (MCP-1), have been shown to modulate the proliferation of monocytic cells. The Th2 cytokine IL-4 has been shown to drive local proliferation of macrophages in helminth-induced inflammation responses (22). Interestingly, we found the IL-4 receptor alpha (IL-4Rα) is expressed on ATMs (Fig. S6*A*). To test whether ATM proliferation could be caused by IL-4, we i.p. injected recombinant IL-4 (23) into lean mice and performed the EdU incorporation assay and Ki67 staining 48 h later. We found that the EdU-incorporated ATMs (Fig. 4*A*) and Ki67^{+} ATMs (Fig. 4*B*) are induced dramatically by IL-4 treatment. It should be noted that the incorporation of such thymidine analog was not detectable in blood monocytes (22). Macrophage differentiation and proliferation also can be regulated by M-CSF in native or inflammatory status (24–26). We examined the expression of colony-stimulating factor 1 receptor (CSF-1R), a specific M-CSF receptor, on cells of the monocytic lineage and found that it was high on peritoneal macrophages as well as monocytes in adipose tissue but not on ATMs of either lean or obese mice (Fig. S6 *A* and *B*). Thus, the proliferation of ATMs is unlikely to be related to M-CSF. A recent report suggested that MCP-1 regulates the local proliferation of ATMs (27). To examine further the effect of M-CSF and MCP-1 on ATM proliferation, we i.p. injected M-CSF and MCP-1 at different concentrations into

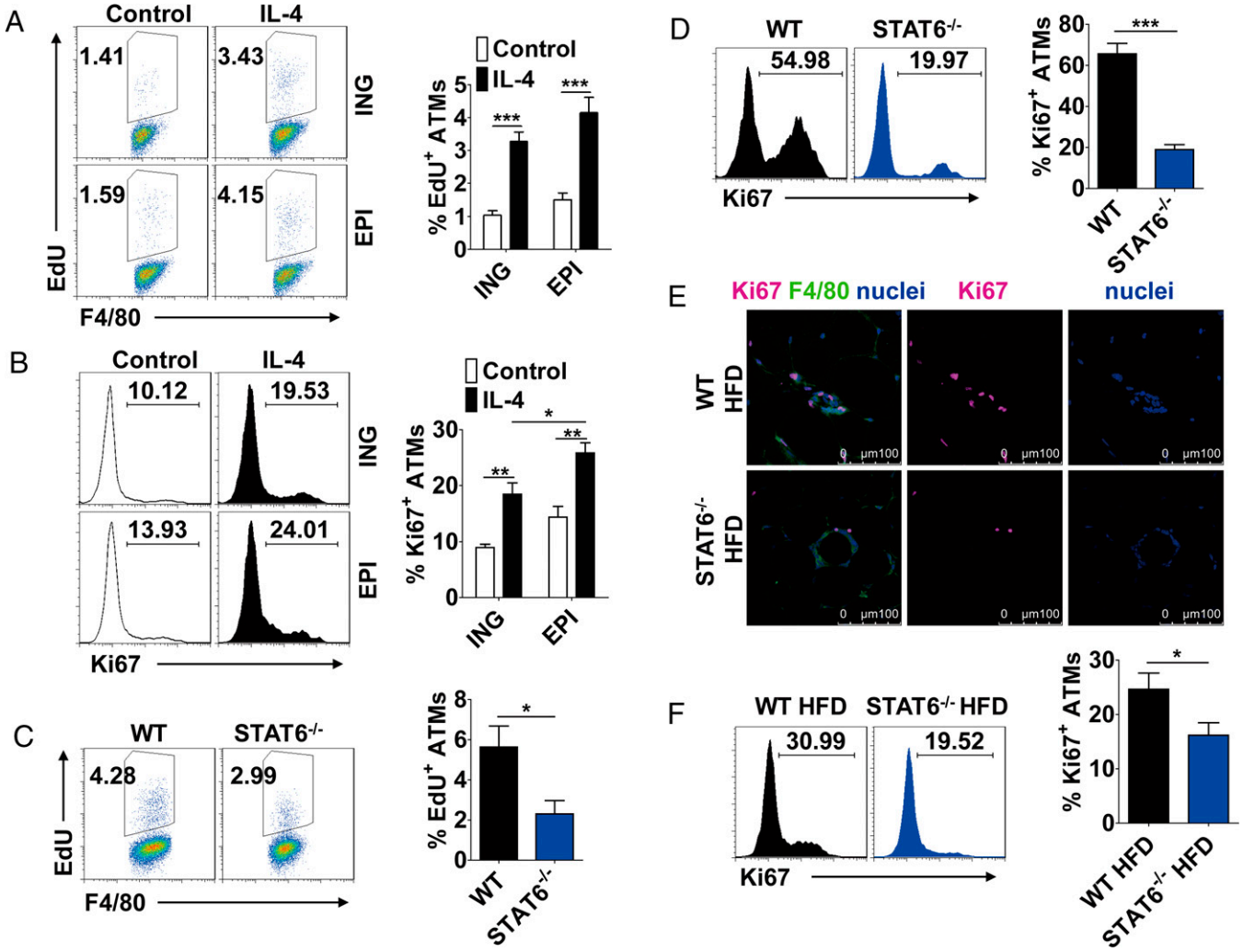

Fig. 4. Proliferation of ATMs depends on the IL-4/STAT6 signaling axis. (*A* and *B*) EdU incorporation (*A*) and Ki67 expression in ATMs (*B*) from the inguinal (ING) and epididymal (EPI) adipose tissue of mice treated for 48 h with saline or the complex of IL-4 and anti–IL-4 (to prolong the bioavailability of IL-4 in vivo) (n = 4–5 mice in each group). (*C* and *D*) EdU incorporation (*C*) and Ki67 expression (*D*) in ATMs from the epididymal adipose tissue of wild-type or STAT6$^{-/-}$ mice treated with the complex of IL-4 and anti–IL-4 for 48 h (n = 6 mice in each group). (*E*) Immunofluorescence staining for Ki67^{+} ATMs in epididymal adipose tissue of wild-type and STAT6$^{-/-}$ mice on an HFD. (Scale bars, 100 μM.) (*F*) Ki67 expression in ATMs from the epididymal adipose tissue of wild-type and STAT6$^{-/-}$ mice on an HFD (n = 6 mice in each group). All bar graphs are presented as means ± SEM. *P < 0.05, **P < 0.01, ***P < 0.001.

lean mice. Forty-eight hours later, myeloid cells in the peripheral blood were significantly induced by either cytokine (Fig. S6*C*), possibly because of recruitment and maturation (28, 29). However, we did not find significant increase when the EdU incorporation assay was performed on ATMs, (Fig. S6*D*). These results indicate that IL-4, but not MCP-1 or M-CSF, could be the cytokine that leads to ATM proliferation.

Upon binding to IL-4, IL-4R recruits STAT6 and IRS2 to mediate the mitogenic activity in lymphocytes. In this process, STAT6 plays a key role (30, 31). To determine the role of IL-4 in ATM proliferation in vivo, we used STAT6$^{-/-}$ mice and performed EdU incorporation and Ki67 expression assays upon IL-4 injection. We found that EdU incorporation (Fig. 4*C*) and Ki67 expression (Fig. 4*D*) were reduced dramatically in STAT6$^{-/-}$ mice compared with wild-type controls. This experiment demonstrated that STAT6 plays a critical role in the IL-4–induced proliferation of ATMs. To verify further whether the IL-4/STAT6 signaling axis plays a role in ATM proliferation during obesity, we treated STAT6$^{-/-}$ mice and wild-type mice with an HFD and similarly assayed ATM proliferation by Ki67 expression. Again, there were significantly fewer Ki67^{+} ATMs in the adipose tissue of STAT6$^{-/-}$ mice than in the adipose tissue of wild-type mice (Fig. 4 *E* and *F*). Thus, the IL-4/STAT6 axis is required for obesity-associated ATM proliferation.

CD11b Restricts IL-4–Induced Macrophage Proliferation and Alternative Activation. Because the CD11b$^{-/-}$ ATMs have increased proliferation in the obesity state, we wondered whether the IL-4 level is augmented in the adipose tissue of CD11b$^{-/-}$ mice. Eosinophils are competent in IL-4 production and have a relatively high proportion in adipose tissue (32). However, we did not find a significant difference in eosinophils in the adipose tissue of CD11b$^{-/-}$ and wild-type mice (Fig. 5*A* and Fig. S2*A*), nor did we find a significant difference in the levels of the IL-4 protein (Fig. 5*B*) or of another Th2 cytokine, IL-13, which also can drive the proliferation of macrophages through the IL-4R/STAT6 pathway (Fig. S7*A*), in the adipose tissues. Therefore, we hypothesize that CD11b$^{-/-}$ ATMs are hyperresponsive to IL-4–induced proliferation. To test this notion, we injected the complex of recombinant IL-4 and anti–IL-4 into lean wild-type and CD11b$^{-/-}$ mice and found that the percentage of EdU-incorporating ATMs was significantly higher in CD11b$^{-/-}$ than in wild-type mice (Fig. 5*C*). It should be noted that

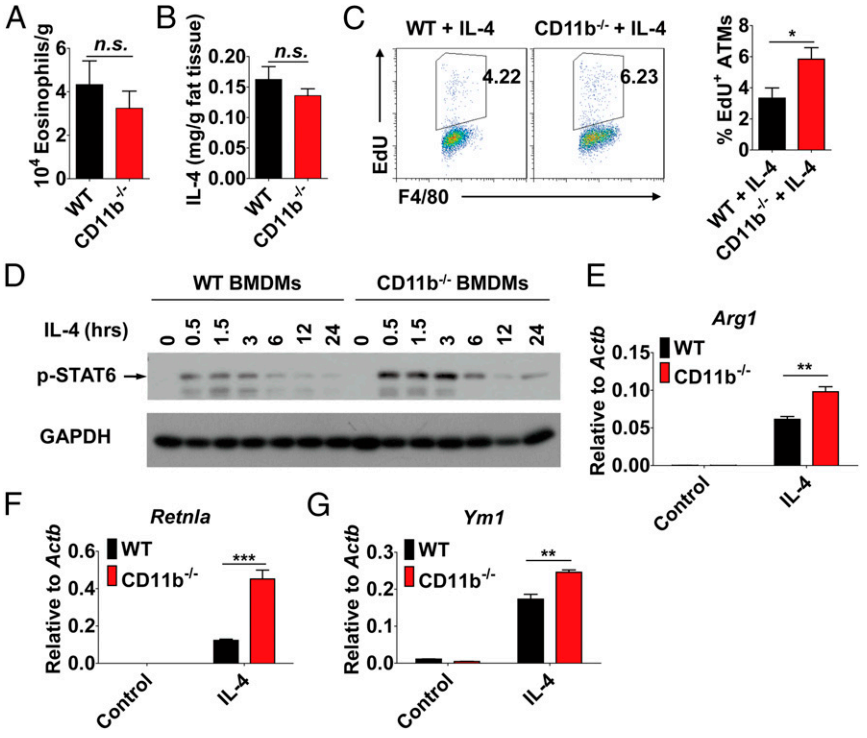

Fig. 5. CD11b restrains IL-4–induced macrophage proliferation and alternative activation. (*A*) The total number of eosinophils per gram of epididymal adipose tissue from HFD-treated mice was analyzed by flow cytometry (n = 4 mice in each group). (*B*) IL-4 levels in epididymal adipose tissue from HFD-treated mice were measured by ELISA (n = 5 mice in each group). (*C*) EdU incorporation in ATMs from the epididymal adipose tissue of wild-type and CD11b$^{-/-}$ mice treated for 48 h with the complex of IL-4 and anti–IL-4 (n = 5 mice in each group). (*D*) Immunoblotting analysis of phosphorylated STAT6 in lysates of wild-type and CD11b$^{-/-}$ BMDMs stimulated with IL-4 (20 ng/mL) for different times. (*E*–*G*) The expression of *Arg1* (*E*), *Retnla* (*F*), and *Ym1* (*G*) in wild-type and CD11b$^{-/-}$ BMDMs untreated or treated for 12 h with 10 ng/mL IL-4 (four repeated wells representing two independent experiments). Data are shown as means ± SEM in *A*, *B*, *C*, *E*, *F*, and *G*. *P < 0.05, **P < 0.01, ***P < 0.001.

the level of IL-4Rα is indistinguishable in wild-type and CD11b$^{-/-}$ ATMs (Fig. S7*B*).

These results suggest that CD11b has an effect on the IL-4/STAT6 signaling axis in macrophages. To investigate the role of CD11b on IL-4/STAT6 signaling, we prepared bone marrow-derived macrophages (BMDMs) from wild-type and CD11b$^{-/-}$ mice. Although the IL-4Rα levels are equal on BMDMs from either type of mice (Fig. S7*C*), the CD11b$^{-/-}$ macrophages exhibited greatly increased phosphorylation of STAT6 when treated with IL-4 (Fig. 5*D* and Fig. S7*D*).

In addition to regulating proliferation, Th2 cytokines are well known for their ability to drive alternative activation of macrophages via STAT6 (6, 33). Therefore, we examined the markers of AAMs and found that in the presence of IL-4 *Arginase I* (*Arg1*), *Retnla*, and *Ym1* are significantly higher in CD11b$^{-/-}$ BMDMs than in those derived from control mice (Fig. 5 *E*–*G*).

CD11b Constrains the IL-4/STAT6 Axis Through Phosphatase SHP-1. The upstream kinases that transduce signals from IL-4–IL-4R to STAT6 are JAK1 and JAK3. We thus examined the status of JAK1 and JAK3 induced by IL-4 and found that indeed the phosphorylation of both JAK1 and JAK3 was increased significantly in the CD11b$^{-/-}$ BMDMs compared with that in wild-type BMDMs (Fig. 6*A* and Fig. S7*D*). Therefore, CD11b may control IL-4 signaling in macrophages in a JAK-dependent manner. It should be noted that in these macrophages the phosphorylation of JAK1 is much lower than that of JAK3 (34). In agreement with the increased IL-4 signaling strength in CD11b-deficient macrophages, blockage of CD11b by antibody, M1/70, also enhanced IL-4–induced phosphorylation of JAK1, JAK3, and STAT6 (Fig. 6*B*). The IL-4–induced expression of *Arg1* also was elevated by CD11b blockage (Fig. 6*C*).

One of the key events in the initiation of integrin CD11b signaling is the activation of Src family kinases (SFKs). To explore whether CD11b-induced SFK activation is involved in the inhibition of the IL-4/STAT6 pathway, we pretreated BMDMs with the SFK inhibitor PP2 and found that it increased the IL-4–induced phosphorylation of JAK3 and STAT6 in wild-type but not in CD11b$^{-/-}$ BMDMs (Fig. 6*D*). Furthermore, *Arg1* expression induced by IL-4 was increased by the inhibition of SFKs in wild-type (Fig. 6*E*) but not in CD11b$^{-/-}$ BMDMs (Fig. S7*E*). These results indicate that SFKs or downstream components participate in the inhibition of IL-4/STAT6 signaling by CD11b.

The JAK–STAT pathways are tightly controlled by phosphatase SHP-1, which directly suppresses the IL-4–STAT6 signaling (35, 36). To examine whether SHP-1 participates in the inhibition of STAT6 phosphorylation by CD11b, we prepared BMDMs from *me^{v}*/*me^{v}* mice, which possess mutated SHP-1 with substantially reduced protein tyrosine phosphatase (PTP) activity (37). In wild-type BMDMs, the phosphorylation of JAK3 and STAT6 induced by IL-4 was increased further by blocking CD11b with M1/70; however, such enhancement did not happen in *me^{v}*/*me^{v}* BMDMs (Fig. 6*F*). These findings suggest that the inhibition of the IL-4/STAT6 pathway by integrin CD11b depends on SHP-1. Although these studies on the signaling process were not designed to delineate the sequential order of JAKs, SFKs, and SHP-1, our results do indicate that CD11b has critical roles in negatively regulating the IL-4 signaling process.

Alternatively Activated ATMs Reverse Insulin Resistance in CD11b-Deficient Mice. Because our data clearly showed that macrophage accumulation and alternative activation can be regulated by CD11b, we further investigated the relevance of such changes in macrophages to insulin resistance. In HFD-induced obesity, we found that the percentage of RELM-α^{+} ATMs was dramatically higher in CD11b$^{-/-}$ mice than in wild-type mice (Fig. 7*A*). We also sorted the ATMs from HFD-induced obese mice and examined the mRNA level of *Arg1*, *Ym1*, *Ppard*, *Gas6*, *Lyve1*, and *Pdgfc*, the markers for alternatively activated macrophages. The expression of these markers was significantly higher in CD11b$^{-/-}$ ATMs than in wild-type ATMs (Fig. 7 *B* and *C* and Fig. S8*A*), indicating increased AAMs in adipose tissue of CD11b$^{-/-}$ mice.

Liver Kupffer cells are typical tissue macrophages that also have been reported to regulate insulin resistance (9). We therefore determined whether the CD11b inhibition of IL-4/STAT6 signaling also could affect the alternative polarization of Kupffer cells. When

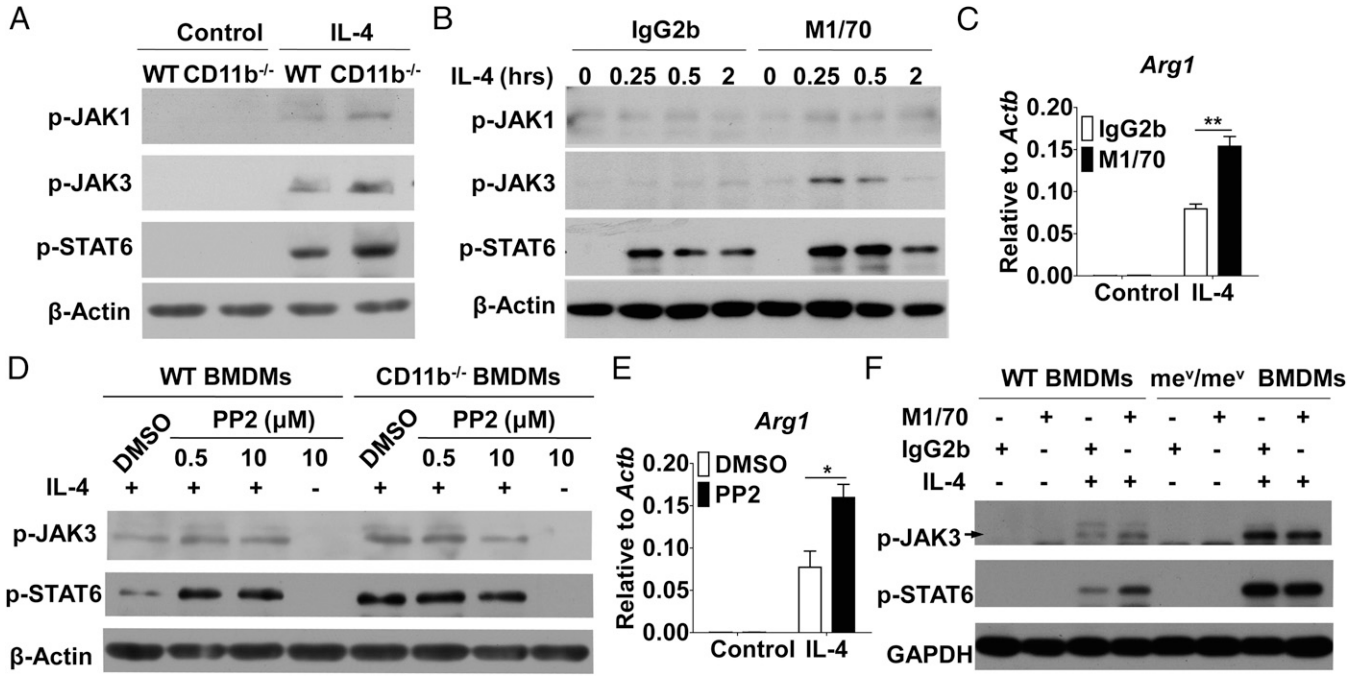

Fig. 6. Integrin CD11b inhibits the IL-4/STAT6 signaling axis through SHP-1. (*A*) Immunoblotting analysis of phosphorylated JAK1, JAK3, and STAT6 in lysates of wild-type and CD11b$^{-/-}$ BMDMs stimulated with 20 ng/mL IL-4 for 30 min or not stimulated (Control). (*B*) Immunoblotting analysis of phosphorylated JAK1, JAK3, and STAT6 in lysates of BMDMs. Wild-type BMDMs were pretreated with CD11b-blocking antibody (M1/70) or isotype (rat IgG2b) and were stimulated with 20 ng/mL IL-4 for 0–2 h. (*C*) The expression of *Arg1* in BMDMs. Wild-type BMDMs were pretreated with M1/70 or IgG2b and were stimulated with 10 ng/mL IL-4 for 12 h or were not stimulated. (*D*) Immunoblotting analysis of phosphorylated JAK3 and STAT6 in lysates of wild-type and CD11b$^{-/-}$ BMDMs. BMDMs were stimulated with 20 ng/mL IL-4 for 30 min after pretreatment with PP2 (0.5 μM or 10 μM for 1 h) or solvent (Control). (*E*) The expression of *Arg1* in BMDMs. Wild-type BMDMs were stimulated with 10 ng/mL IL-4 for 12 h after pretreatment with PP2 (10 μM for 1 h) or solvent (Control). (*F*) Immunoblotting analysis of phosphorylated JAK3 and STAT6 in wild-type and *me^{v}/me^{v}* BMDMs. BMDMs were pretreated with M1/70 or IgG2b before being stimulated for 30 min with 20 ng/mL IL-4. Data in *C* and *E* are shown as means ± SEM of three or four replicates representing two independent experiments. *$P < 0.05$, **$P < 0.01$.

the expression of ARG-1 in Kupffer cells was analyzed by flow cytometry, we could not detect significant difference between wild-type and CD11b-deficient mice (Fig. S8*B*). We also examined the expression of several other markers of AAMs (*Clec10a*, *Clec7a*, *Il1rn*, *Jag1*, *Mrc1*, *Pdcd1lg*, *Ppard*, *Retnla*, and *Ym1*) in liver and found no significant difference between wild-type and CD11b-deficient mice (Fig. S8*C*). It has been reported that the expression of CD11b on Kupffer cells is very low (38), and we also found that the level of CD11b is more than sevenfold lower on Kupffer cells than on ATMs (Fig. S8*D*). Because of its low level of expression on Kupffer cells, CD11b has much less effect on Kupffer cells than on ATMs.

CD11b also is expressed on eosinophils, neutrophils, and natural killer (NK) cells. The infiltration of those cells into adipose tissue has also relevance to obesity-related insulin resistance (32, 39, 40). Specifically, eosinophils improve insulin resistance by secreting IL-4 that promotes alternative activation of ATMs, neutrophils mediate insulin resistance by producing elastase, and NK cells contribute to insulin resistance by releasing IFN-γ (32, 39, 40). We therefore examined these cells in epididymal adipose tissue. We did not find any difference in the number of these cells per gram of adipose tissue from wild-type and CD11b$^{-/-}$ mice (Fig. 5*A* and Figs. S2*A* and S8 *E* and *F*), nor did we find difference in the expression of IL-4, neutrophil elastase (*Elane*), or IFN-γ (Fig. S8 *G–I*).

Gut microbiota have been shown to be involved in the development of obesity and metabolic abnormalities (41). It also has been reported that there is an increase in the abundance of bacteria belonging to the phylum Firmicutes and a decrease in the abundance of bacteria in the phylum Bacteroidetes in obese humans and mice (42). To investigate whether microbiota play a role in the development of metabolic abnormalities associated with CD11b status, we examined the abundance of fecal bacteria in these two phyla in CD11b-deficient and wild-type mice on an HFD using quantitative PCR (qPCR)-based analysis of bacterial 16S rRNA genes. Interestingly, we did not find any significant differences between CD11b-deficient and wild-type mice. We further analyzed in more detail the fecal bacteria that have been reported to be associated with obesity and blood glucose changes. Again, we did not find significant differences between CD11b-deficient and wild-type in the abundance of these bacteria (Fig. S8*J*). Therefore, the reduced insulin resistance in CD11b-deficient mice is not a consequence of altered gut microbiota.

We further investigated whether the increase in the proliferation and alternative activation of ATMs is associated with the reduction in insulin resistance in the paradigm of bone marrow reconstitution. As revealed in our immunohistochemical staining, significantly more Ki67^{+} macrophages and RELM-α^{+}macrophages existed in the adipose tissue of CD45.1 mice reconstituted with CD11b$^{-/-}$ bone marrow than in the adipose tissue of CD45.1 mice reconstituted with wild-type bone marrow (Fig. S9 *A–D*), indicating an increase in the proliferation and alternative activation of CD11b$^{-/-}$ ATMs.

Alternatively activated ATMs could alleviate insulin resistance by attenuating the inflammation as well as by improving the metabolic function of adipose tissue (9, 10, 43). To verify the role of alternatively activated ATMs on improved insulin resistance in CD11b$^{-/-}$ mice, we selectively depleted these macrophages by i.p. injection of mannosylated clodronate liposome, which would be specifically incorporated by AAMs in the facilitation of mannose receptors and would induce apoptosis of these cells (44). We did not find a reduction in Kupffer cells after 4 d of treatment with mannosylated clodronate liposome, whereas the RELM-α^{+} ATMs were greatly decreased in both the inguinal adipose tissue and the epididymal adipose tissue of HFD-treated mice (Fig. S9 *E* and *F*).

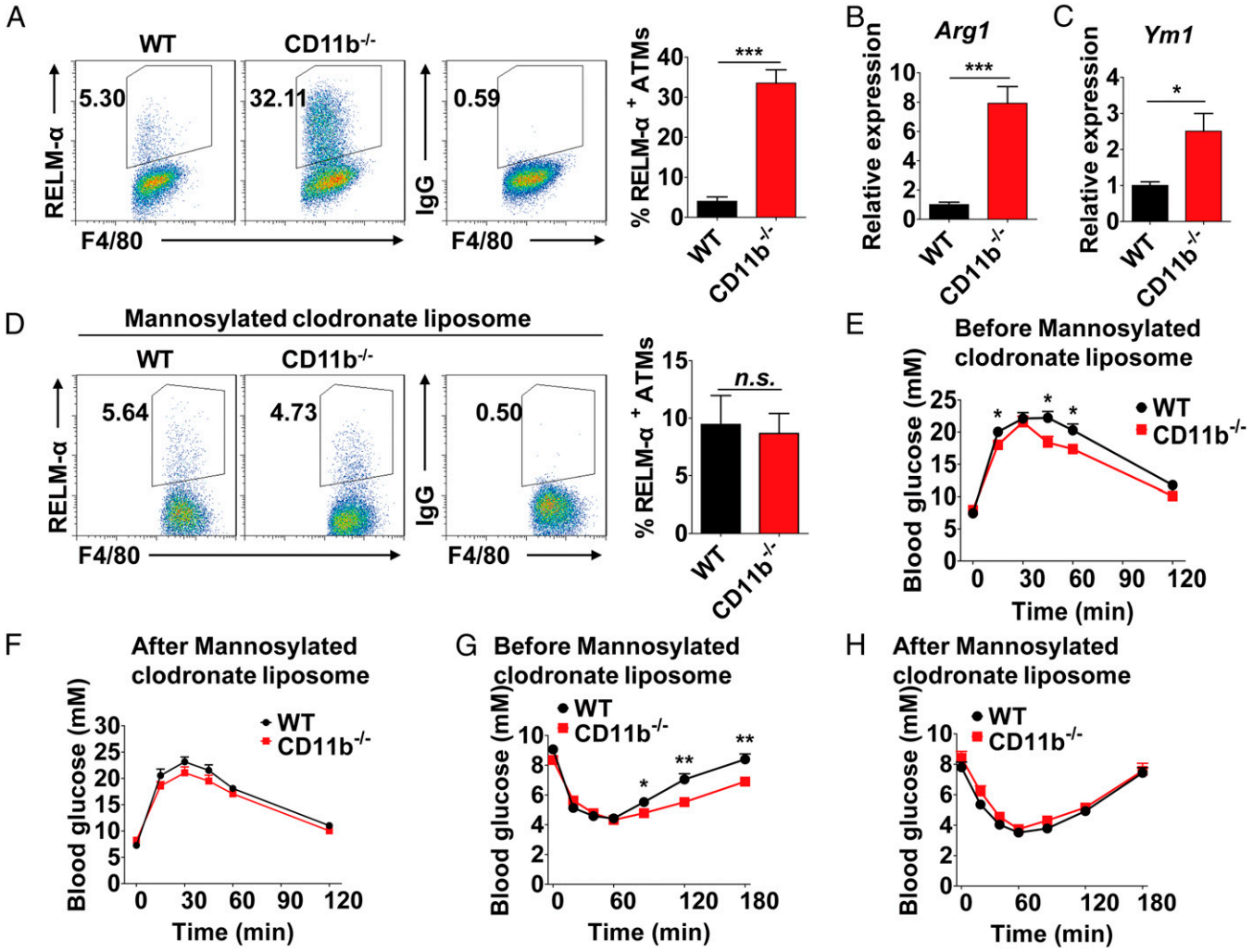

Fig. 7. CD11b promotes insulin resistance by inhibiting alternative activation of ATMs. (*A*) RELM-α expression in ATMs from the epididymal adipose tissue of wild-type and CD11b$^{-/-}$ mice on an HFD ($n = 5$ mice in each group). (*B* and *C*) Relative expression of *Arg1* (*B*) and *Ym1* (*C*) in sorted ATMs from the epididymal adipose tissue of wild-type and CD11b$^{-/-}$ mice on an HFD ($n = 4$ mice in each group). (*D*) RELM-α expression in ATMs from the epididymal adipose tissue of HFD-treated wild-type or CD11b$^{-/-}$ mice after treatment with 1 mg mannosylated clodronate liposome. (*E* and *F*) Glucose-tolerance test in HFD-treated wild-type and CD11b$^{-/-}$ mice before (*E*) and after (*F*) treatment with 1 mg mannosylated clodronate liposome ($n = 9$–10 mice in each group). Error bars represent means ± SEM. *$P < 0.05$. (*G* and *H*) Insulin-tolerance test in HFD-treated wild-type and CD11b$^{-/-}$ mice before (*G*) and after (*H*) treatment with 1 mg mannosylated clodronate liposome ($n = 9$–10 mice in each group). Error bars represent means ± SEM. *$P < 0.05$, **$P < 0.01$.

When similar treatment was used in HFD-treated wild-type or CD11b$^{-/-}$ mice, we found that the RELM-α^{+} ATMs were equally reduced (Fig. 7*D*). Significantly, the reversal of insulin resistance in CD11b$^{-/-}$ mice disappeared (Fig. 7 *E*–*H*). Thus, CD11b modulates insulin resistance by affecting AAMs.

Discussion

ATM accumulation is a key feature of obesity-associated chronic inflammation. These cells could promote further metabolic disorders such as insulin resistance (45). However, the mechanisms underlining macrophage accumulation in adipose tissue and the function of different macrophage phenotypes have yet to be defined. CD11b is well known for its role in regulating leukocyte migration and adhesion. Our study unveiled previously unidentified aspects of CD11b in regulating the accumulation and function of macrophages in adipose tissue during HFD-induced obesity. Indeed, we found that CD11b is important in mediating monocyte immigration into adipose tissue. Without CD11b, there is an increase in the in situ proliferation as well as in the alternative activation of ATMs and reduced insulin resistance. In this scenario, it is likely that the promotion of the alternatively activated phenotype is the key to the metabolic phenotype associated with CD11b deficiency. As a consequence of the enhanced in situ proliferation of ATMs, the number of AAMs is augmented, and thus the effect of these cells is amplified. Therefore we believe the improved insulin resistance in CD11b-deficient mice is a synergistic effect of the enhanced in situ proliferation of ATMs and the promotion of alternatively activated ATMs.

It is believed that ATMs are derived from circulating monocytes (3). Recent studies suggest that macrophages in various tissues can be maintained autonomously, and their precursors may not come from bone marrow (46). In some tissues, macrophages are able to self-renew and proliferate locally in a static state, as demonstrated for microglia (47, 48), Kupffer cells (49), and Langerhans cells (50). During acute inflammation such as that induced by parasitic infections, the local proliferation of macrophages is promoted dramatically by Th2 cytokines, and these cells possess an alternative activation phenotype (22). In low-grade and chronic inflammation, such as atherosclerosis, macrophage accumulation likely is determined by local proliferation (51). However, there is only limited information about the origin and proliferation of ATMs (27, 52,

53). We systemically examined the immigration and proliferation of ATMs in wild-type and CD11b-deficient mice. Our study demonstrated that in situ macrophage proliferation contributes greatly to ATM accumulation, especially in the absence of CD11b. In CD11b-deficient mice, we found that, although there is a fourfold reduction in the immigration of blood monocytes into adipose tissue, the ATM accumulation is much higher. Indeed, we found much stronger proliferation of macrophages in the adipose tissue of CD11b-deficient mice, as demonstrated by the EdU incorporation assay and the analysis of Ki67 expression.

Various factors, such as M-CSF and Th2 cytokines, have been reported to regulate macrophage proliferation (22, 24). Instead, upon the addition of exogenous IL-4, the proliferation of ATMs could be boosted dramatically, a process that depends on STAT6 signaling. In support of the role of an IL-4–induced signaling process, the obesity-associated macrophage proliferation was greatly decreased in STAT6-deficient mice. It has been reported that several cell types in the adipose tissue, e.g. Th2 cells (54), eosinophils (32), and adipocytes themselves (10), are capable of producing IL-4. It has been reported that the initiation of obesity is concomitant with an evoked Th2 immune response in adipose tissue characterized by increased IL-4 expression and alternative activation of macrophages (55). Interestingly, the IL-4 level also is increased in obese patients (56). Although the aim of this investigation was not to identify the cell types that produce IL-4, we did find that IL-4 signaling is required and that in vivo administration of IL-4 could promote further ATM proliferation.

The mitogenic property of IL-4 often is investigated in the context of IL-4R expression. We found that CD11b deficiency promotes IL-4–induced ATM proliferation; i.e., CD11b could provide a negative effect on the mitogenic signal of IL-4. Although the exact mechanism of the CD11b-regulated IL-4 signaling process remains to be elucidated, we did show that members of Src family kinases and SHP-1 are indispensable for this effect. The activation of members of Src family kinases, one of the earliest events in integrin signaling, has dual effects on the signal transduction of immune receptors, phosphorylating both immunoreceptor tyrosine-based activation motifs (ITAMs) and immunoreceptor tyrosine-based inhibitory motifs (ITIMs) (57). Interestingly, IL-4Rα possesses an ITIM domain on the C terminal that has been reported to recruit SHP-1, which in turn down-regulates the IL-4–initiated signaling process (58). Based on this information, we propose the following model: Signals from CD11b activate members of Src family kinases, and those kinases further phosphorylate the ITIM domain on IL-4Rα, leading to the recruitment of SHP-1 to suppress IL-4/STAT6 signaling. Although this model seems to explain our data logically, the exact hierarchy of these molecules requires more detailed investigation.

In summary, our study demonstrates that integrin CD11b negatively regulates IL-4/STAT6–induced proliferation of ATMs and the polarization of the alternatively activated phenotype. This effect of CD11b likely depends on a complex signaling process involving members of the Src family kinases and SHP-1. This function of CD11b not only provides insights into the physiological function of integrins but also has important implications for designing new therapeutic strategies for obesity-related insulin resistance.

Materials and Methods

Animal Experiments. C57BL/6 and BALB/c mice were purchased from the Shanghai Laboratory Animal Center of the Chinese Academy of Sciences. CD11b$^{-/-}$ mice were backcrossed with the C57BL/6 mice as described previously (14). STAT6$^{-/-}$ (C.129S2-Stat6^{tm1Gru}/J) and *me^{v}*/*me^{v}* (C57BL/6J-Ptpn6$^{me\text{-}v}$/J) mice were from Jackson Laboratory. CD45.1 C57BL/6 mice were kindly provided by Yanyun Zhang of the Institute of Health Sciences of the Chinese Academy of Sciences in Shanghai, China. All experiments were approved by the Institutional Animal Care and Use Committee of the Institute of Health Sciences, Shanghai Institutes for Biological Sciences of Chinese Academy of Sciences.

HFD-induced obesity was induced by feeding male mice with a diet containing 60 kcal% fat (D12492; Research Diets) starting at age 5 wk. The control group was fed with a normal chow diet. All experimental analyses were performed after mice were fed an HFD for 8–10 wk. Glucose-tolerance tests were carried out with i.p. injection of 1 g glucose per kilogram of body weight, and insulin-tolerance tests were carried out with i.p. injection of 0.75 U insulin per kilogram of body weight. The serum insulin level was measured by a multiplex immunoassay using the Bio-Plex technology (Bio-Rad). To compare the migration capacity of monocytes, CD11b$^{-/-}$ and wild-type monocytes were isolated from bone marrow with a negative selection kit (Stemcell Technologies), and either CD11b$^{-/-}$ and wild-type monocytes in a 1:1 ratio or CD11b$^{-/-}$ monocytes alone were i.v. injected into HFD-treated CD45.1 mice. The EdU incorporation assay was carried out with the Click-iT EdU assay kit (Life Technologies). Mice were i.p. injected with 10 μg EdU per gram of body weight and were killed 3 h later. Adipose tissue was collected, and the Click-iT reaction was performed and analyzed flow cytometrically and immunohistologically according to the manufacturer's instruction. To examine the role of MCP-1, M-CSF, and IL-4 in ATMs proliferation, 0.1 or 1 μg MCP-1 (Life Technologies), 1 or 10 μg mouse M-CSF (R&D Systems), a complex of 5 μg IL-4 (PeproTech) and 25 μg IL-4 antibody (clone 11B11; Harlan Bioproducts for Science), or PBS was i.p. injected into mice, and ATMs analysis was performed 48 h later. For depletion of AAMs, HFD-treated mice were i.p. injected with 1 mg mannosylated clodronate liposome (Encapsula NanoSciences). The glucose-tolerance test and analysis of ATMs were carried out between day 4 and day 8.

Flow Cytometric Analysis of Cellular Proteins. Adipose tissues were cut into small pieces, rinsed with PBS, and digested with 2 mg/mL collagenase I (Sigma-Aldrich) for 1 h. The cell suspensions were filtered through 70-μm sieves and centrifuged to separate adipocytes. The cell pallets were resuspended and subjected to erythrocyte lysis. The cell suspension then was preincubated with anti-CD16/CD32 (eBioscience) to block Fc receptors before surface molecule staining. The antibodies used to detect surface proteins including CD3e, CD4, CD8a, CD19, NK1.1, F4/80, CD45, CD11b, CD45.1, CD45.2, Ki67, and Ly6C were from eBioscience, and those for CD115, Ly6G, and Siglec-F were from BioLegend. Anti–IL-4Rα was from R&D Systems.

For intracellular RELM-α staining in ATMs, GolgiPlug (BD Biosciences) was added to collagenase in a 1:1,000 ratio before digestion. After staining of surface molecules, intracellular staining was performed with fixation and permeabilization kits according to the manufacturer's instructions (eBioscience). Rabbit anti–RELM-α (Abcam) and Alexa Fluor 647-conjugated donkey anti-rabbit IgG (Life Technologies) were used.

Immunohistology. Adipose tissues were cut into small pieces and fixed in 4% paraformaldehyde for 24 h at 4 °C before whole-mount staining. Briefly, the specimen was permeabilized with 1% Triton X-100, blocked with 1% BSA and 3% FBS in PBS, then stained with Alexa Fluor 488-conjugated rat anti-F4/80 mAbs (eBioscience) and Alexa Fluor 647-conjugated rat anti-Ki67 mAbs (eBioscience). The nuclei were counterstained with Hoechst 33342 (Life Technologies). The adipocytes were counterstained with BODIPY 558/568 C_{12} (Life Technologies). The TUNEL assay was performed on paraffin-embedded adipose tissue sections with an in situ cell-death detection kit (Roche Applied Science).

BMDMs. Bone marrow cells were isolated from femurs and tibias of CD11b$^{-/-}$ and wild-type mice and then were cultured in DMEM/F12 medium with the addition of 10% (vol/vol) FBS and 20% (vol/vol) L929 conditioned medium for 7 d. For CD11b blockage, BMDMs were pretreated with either 20 μg/mL CD11b antibodies M1/70 (eBioscience) or 20 μg/mL rat IgG2b (eBioscience) at room temperature for 1 h before plating. For inhibition of SFKs, BMDMs were treated with DMSO or PP2 (at a concentration of 0.5 μM or 10 μM) for 1 h and were stimulated with IL-4 (PeproTech) 1 h later.

Immunoblotting Assay. Cells were lysed with radioimmunoprecipitation assay (RIPA) lysis buffer (Millipore) supplemented with protease inhibitor mixtures (Roche Applied Science). Proteins were separated by SDS/PAGE and were transferred onto nitrocellulose or PVDF membrane. The antibodies specific for STAT6 phosphorylated at Tyr641 (ab54461) were from Abcam. Antibodies specific for JAK1 phosphorylated at Tyr1022 and Tyr1023 (3331), JAK3 phosphorylated at Tyr980 and Tyr981 (5031), JAK1 (3344), and GAPDH (2118) were from Cell Signaling Technology. Antibody against total STAT6 (sc-1689) was from Santa Cruz Biotechnology. The monoclonal anti–β-Actin (A2228) was from Sigma-Aldrich.

Gene Expression Analysis. Real-time qPCR was performed with the 7900 HT Fast Real-Time PCR system (Life Technologies) using FastStart Universal SYBR Green Master (Roche Applied Science). Oligonucleotide primers were as follows: *Arg1*, 5′-CTCCAAGCCAAAGTCCTTAGAG-3′, 5′-AGGAGCTGTCATTAGGGACATC-3′; *Retnla*, 5′-GGATGCCAACTTTGAATAGGA-3′, 5′-GGATAGTTAGCTGGATTGGCA-3′; *Ym1*, 5′-CAGGTCTGGCAATTCTTCTGAA-3′, 5′-GTCTTGCTCATGTGTGTAAGTGA3′; and *Actb*, 5′-CCACGAGCGGTTCCGATG-3′, 5′-GCCACAGGATTCCATACCCA-3′.

Statistical Analysis. Data are presented as means ± SEM. Significance was assessed by an unpaired two-tailed *t*-test unless otherwise indicated. We considered $P < 0.05$ as statistically significant.

ACKNOWLEDGMENTS. We thank Dr. Douglas Green, Dr. Guang Ning, Dr. Xiangyin Kong, and Dr. Jiqiu Wang for comments and suggestions and Dr. Yanyun Zhang for providing CD45.1 mice. This study was supported by Grant XDA 01040100 from the Scientific Innovation Project of the Chinese Academy of Science; Grant 2015CB964400 from the Ministry of Science and Technology of China; National Natural Science of China Programs 81330046, 81273316, 81530043, and 81571612; the External Cooperation Program of Bureau of International Co-operation, Grant GJHZ201307 from the Chinese Academy of Sciences; Grant 12JC1409200 from the Shanghai Municipal Key Projects of Basic Research; Shanghai Rising-Star Program 14QA1404200; and Grant 12ZR1452600 from the Shanghai Municipal Natural Science Foundation.

1. Hotamisligil GS, Shargill NS, Spiegelman BM (1993) Adipose expression of tumor necrosis factor-alpha: Direct role in obesity-linked insulin resistance. *Science* 259(5091): 87–91.
2. Uysal KT, Wiesbrock SM, Marino MW, Hotamisligil GS (1997) Protection from obesity-induced insulin resistance in mice lacking TNF-alpha function. *Nature* 389(6651): 610–614.
3. Weisberg SP, et al. (2003) Obesity is associated with macrophage accumulation in adipose tissue. *J Clin Invest* 112(12):1796–1808.
4. Xu H, et al. (2003) Chronic inflammation in fat plays a crucial role in the development of obesity-related insulin resistance. *J Clin Invest* 112(12):1821–1830.
5. Gordon S, Taylor PR (2005) Monocyte and macrophage heterogeneity. *Nat Rev Immunol* 5(12):953–964.
6. Gordon S, Martinez FO (2010) Alternative activation of macrophages: Mechanism and functions. *Immunity* 32(5):593–604.
7. Gordon S (2003) Alternative activation of macrophages. *Nat Rev Immunol* 3(1):23–35.
8. Lumeng CN, Bodzin JL, Saltiel AR (2007) Obesity induces a phenotypic switch in adipose tissue macrophage polarization. *J Clin Invest* 117(1):175–184.
9. Odegaard JI, et al. (2007) Macrophage-specific PPARgamma controls alternative activation and improves insulin resistance. *Nature* 447(7148):1116–1120.
10. Kang K, et al. (2008) Adipocyte-derived Th2 cytokines and myeloid PPARdelta regulate macrophage polarization and insulin sensitivity. *Cell Metab* 7(6):485–495.
11. Springer TA, Anderson DC (1986) The importance of the Mac-1, LFA-1 glycoprotein family in monocyte and granulocyte adherence, chemotaxis, and migration into inflammatory sites: Insights from an experiment of nature. *Ciba Found Symp* 118: 102–126.
12. Issekutz TB (1995) In vivo blood monocyte migration to acute inflammatory reactions, IL-1 alpha, TNF-alpha, IFN-gamma, and C5a utilizes LFA-1, Mac-1, and VLA-4. The relative importance of each integrin. *J Immunol* 154(12):6533–6540.
13. Abram CL, Lowell CA (2009) The ins and outs of leukocyte integrin signaling. *Annu Rev Immunol* 27:339–362.
14. Ehirchiou D, et al. (2007) CD11b facilitates the development of peripheral tolerance by suppressing Th17 differentiation. *J Exp Med* 204(7):1519–1524.
15. Han C, et al. (2010) Integrin CD11b negatively regulates TLR-triggered inflammatory responses by activating Syk and promoting degradation of MyD88 and TRIF via Cbl-b. *Nat Immunol* 11(8):734–742.
16. Yakubenko VP, Bhattacharjee A, Pluskota E, Cathcart MK (2011) αMβ₂ integrin activation prevents alternative activation of human and murine macrophages and impedes foam cell formation. *Circ Res* 108(5):544–554.
17. Ding C, et al. (2013) Integrin CD11b negatively regulates BCR signalling to maintain autoreactive B cell tolerance. *Nat Commun* 4:2813.
18. Dong ZM, Gutierrez-Ramos JC, Coxon A, Mayadas TN, Wagner DD (1997) A new class of obesity genes encodes leukocyte adhesion receptors. *Proc Natl Acad Sci USA* 94(14): 7526–7530.
19. Anderson DC, Springer TA (1987) Leukocyte adhesion deficiency: An inherited defect in the Mac-1, LFA-1, and p150,95 glycoproteins. *Annu Rev Med* 38:175–194.
20. Coxon A, et al. (1996) A novel role for the beta 2 integrin CD11b/CD18 in neutrophil apoptosis: A homeostatic mechanism in inflammation. *Immunity* 5(6):653–666.
21. Mayadas TN, Cullere X (2005) Neutrophil beta2 integrins: Moderators of life or death decisions. *Trends Immunol* 26(7):388–395.
22. Jenkins SJ, et al. (2011) Local macrophage proliferation, rather than recruitment from the blood, is a signature of TH2 inflammation. *Science* 332(6035):1284–1288.
23. Finkelman FD, et al. (1993) Anti-cytokine antibodies as carrier proteins. Prolongation of in vivo effects of exogenous cytokines by injection of cytokine-anti-cytokine antibody complexes. *J Immunol* 151(3):1235–1244.
24. Hashimoto D, et al. (2013) Tissue-resident macrophages self-maintain locally throughout adult life with minimal contribution from circulating monocytes. *Immunity* 38(4): 792–804.
25. Davies LC, et al. (2013) Distinct bone marrow-derived and tissue-resident macrophage lineages proliferate at key stages during inflammation. *Nat Commun* 4:1886.
26. Jenkins SJ, et al. (2013) IL-4 directly signals tissue-resident macrophages to proliferate beyond homeostatic levels controlled by CSF-1. *J Exp Med* 210(11):2477–2491.
27. Amano SU, et al. (2014) Local proliferation of macrophages contributes to obesity-associated adipose tissue inflammation. *Cell Metab* 19(1):162–171.
28. Papatriantafyllou M (2011) Monocytes: Nudged out of the niche. *Nat Rev Immunol* 11(6):368–369.
29. Mossadegh-Keller N, et al. (2013) M-CSF instructs myeloid lineage fate in single haematopoietic stem cells. *Nature* 497(7448):239–243.
30. Wurster AL, Withers DJ, Uchida T, White MF, Grusby MJ (2002) Stat6 and IRS-2 cooperate in interleukin 4 (IL-4)-induced proliferation and differentiation but are dispensable for IL-4-dependent rescue from apoptosis. *Mol Cell Biol* 22(1):117–126.
31. Kaplan MH, Schindler U, Smiley ST, Grusby MJ (1996) Stat6 is required for mediating responses to IL-4 and for development of Th2 cells. *Immunity* 4(3):313–319.
32. Wu D, et al. (2011) Eosinophils sustain adipose alternatively activated macrophages associated with glucose homeostasis. *Science* 332(6026):243–247.
33. Martinez FO, Helming L, Gordon S (2009) Alternative activation of macrophages: An immunologic functional perspective. *Annu Rev Immunol* 27:451–483.
34. Malabarba MG, et al. (1995) Activation of JAK3, but not JAK1, is critical to interleukin-4 (IL4) stimulated proliferation and requires a membrane-proximal region of IL4 receptor alpha. *J Biol Chem* 270(16):9630–9637.
35. Haque SJ, Harbor P, Tabrizi M, Yi T, Williams BRG (1998) Protein-tyrosine phosphatase Shp-1 is a negative regulator of IL-4- and IL-13-dependent signal transduction. *J Biol Chem* 273(51):33893–33896.
36. Kelly-Welch AE, Hanson EM, Boothby MR, Keegan AD (2003) Interleukin-4 and interleukin-13 signaling connections maps. *Science* 300(5625):1527–1528.
37. Shultz LD, et al. (1993) Mutations at the murine motheaten locus are within the hematopoietic cell protein-tyrosine phosphatase (Hcph) gene. *Cell* 73(7):1445–1454.
38. Movita D, et al. (2012) Kupffer cells express a unique combination of phenotypic and functional characteristics compared with splenic and peritoneal macrophages. *J Leukoc Biol* 92(4):723–733.
39. Talukdar S, et al. (2012) Neutrophils mediate insulin resistance in mice fed a high-fat diet through secreted elastase. *Nat Med* 18(9):1407–1412.
40. Wensveen FM, et al. (2015) NK cells link obesity-induced adipose stress to inflammation and insulin resistance. *Nat Immunol* 16(4):376–385.
41. Nicholson JK, et al. (2012) Host-gut microbiota metabolic interactions. *Science* 336(6086):1262–1267.
42. Tremaroli V, Bäckhed F (2012) Functional interactions between the gut microbiota and host metabolism. *Nature* 489(7415):242–249.
43. Vats D, et al. (2006) Oxidative metabolism and PGC-1beta attenuate macrophage-mediated inflammation. *Cell Metab* 4(1):13–24.
44. Miron VE, et al. (2013) M2 microglia and macrophages drive oligodendrocyte differentiation during CNS remyelination. *Nat Neurosci* 16(9):1211–1218.
45. Johnson AMF, Olefsky JM (2013) The origins and drivers of insulin resistance. *Cell* 152(4):673–684.
46. Schulz C, et al. (2012) A lineage of myeloid cells independent of Myb and hematopoietic stem cells. *Science* 336(6077):86–90.
47. Ajami B, Bennett JL, Krieger C, Tetzlaff W, Rossi FMV (2007) Local self-renewal can sustain CNS microglia maintenance and function throughout adult life. *Nat Neurosci* 10(12):1538–1543.
48. Ginhoux F, et al. (2010) Fate mapping analysis reveals that adult microglia derive from primitive macrophages. *Science* 330(6005):841–845.
49. Klein I, et al. (2007) Kupffer cell heterogeneity: Functional properties of bone marrow derived and sessile hepatic macrophages. *Blood* 110(12):4077–4085.
50. Chorro L, et al. (2009) Langerhans cell (LC) proliferation mediates neonatal development, homeostasis, and inflammation-associated expansion of the epidermal LC network. *J Exp Med* 206(13):3089–3100.
51. Robbins CS, et al. (2013) Local proliferation dominates lesional macrophage accumulation in atherosclerosis. *Nat Med* 19(9):1166–1172.
52. Oh DY, Morinaga H, Talukdar S, Bae EJ, Olefsky JM (2012) Increased macrophage migration into adipose tissue in obese mice. *Diabetes* 61(2):346–354.
53. Haase J, et al. (2014) Local proliferation of macrophages in adipose tissue during obesity-induced inflammation. *Diabetologia* 57(3):562–571.
54. Winer S, et al. (2009) Normalization of obesity-associated insulin resistance through immunotherapy. *Nat Med* 15(8):921–929.
55. Prieur X, et al. (2011) Differential lipid partitioning between adipocytes and tissue macrophages modulates macrophage lipotoxicity and M2/M1 polarization in obese mice. *Diabetes* 60(3):797–809.
56. El-Wakkad A, Hassan Nel-M, Sibaii H, El-Zayat SR (2013) Proinflammatory, anti-inflammatory cytokines and adiponkines in students with central obesity. *Cytokine* 61(2):682–687.
57. Berton G, Mócsai A, Lowell CA (2005) Src and Syk kinases: Key regulators of phagocytic cell activation. *Trends Immunol* 26(4):208–214.
58. Nelms K, Keegan AD, Zamorano J, Ryan JJ, Paul WE (1999) The IL-4 receptor: Signaling mechanisms and biologic functions. *Annu Rev Immunol* 17:701–738.